agronomy

MDPI

Article

Transcriptome Analysis and Genome-Wide Gene Family Identification Enhance Insights into Bacterial Wilt Resistance in Tobacco

Zhengwen Liu [1,†], Zhiliang Xiao [1,†], Ruimei Geng [1], Min Ren [1], Xiuming Wu [1], He Xie [2], Ge Bai [2], Huifen Zhang [1], Dan Liu [1], Caihong Jiang [1], Lirui Cheng [1,*] and Aiguo Yang [1,*]

[1] Key Laboratory for Tobacco Gene Resources, Tobacco Research Institute, Chinese Academy of Agricultural Sciences, Qingdao 266101, China; renmin@caas.cn (M.R.)
[2] Yunnan Academy of Tobacco Agriculture Sciences, Kunming 650021, China
* Correspondence: chenglirui@caas.cn (L.C.); yangaiguo@caas.cn (A.Y.)
† These authors contributed equally to this work.

Abstract: Bacterial wilt, caused by the *Ralstonia solanacearum* species complex, is one of the most damaging bacterial diseases in tobacco and other *Solanaceae* crops. In this study, we conducted an analysis and comparison of transcriptome landscape changes in seedling roots of three tobacco BC_4F_5 lines, C244, C010, and C035, with different resistance to bacterial wilt at 3, 9, 24, and 48 h after *R. solanacearum* infection. A number of biological processes were highlighted for their differential enrichment between C244, C010, and C035, especially those associated with cell wall development, protein quality control, and stress response. Hence, we performed a genome-wide identification of seven cell wall development-related gene families and six heat shock protein (Hsp) families and proposed that genes induced by *R. solanacearum* and showing distinct expression patterns in C244, C010, and C035 could serve as a potential gene resource for enhancing bacterial wilt resistance. Additionally, a comparative transcriptome analysis of *R. solanacearum*-inoculated root samples from C244 and C035, as well as C010 and C035, resulted in the identification of a further 33 candidate genes, of which *Nitab4.5_0007488g0040*, a member of the pathogenesis-related protein 1 (PR-1) family, was found to positively regulate bacterial wilt resistance, supported by real-time quantitative PCR (qRT-PCR) and virus-induced gene silencing (VIGS) assays. Our results contribute to a better understanding of molecular mechanisms underlying bacterial wilt resistance and provide novel alternative genes for resistance improvement.

Keywords: tobacco; BC_4F_5 lines; bacterial wilt; transcriptome; gene family; PR-1 protein

Citation: Liu, Z.; Xiao, Z.; Geng, R.; Ren, M.; Wu, X.; Xie, H.; Bai, G.; Zhang, H.; Liu, D.; Jiang, C.; et al. Transcriptome Analysis and Genome-Wide Gene Family Identification Enhance Insights into Bacterial Wilt Resistance in Tobacco. *Agronomy* **2024**, *14*, 250. https://doi.org/10.3390/agronomy14020250

Academic Editor: Maria Céu Lavado da Silva

Received: 13 December 2023
Revised: 20 January 2024
Accepted: 22 January 2024
Published: 24 January 2024

1. Introduction

Tobacco is an important economic crop in the world, and also a useful tool for investigating a range of cytogenetic and molecular genetic issues. At present, tobacco is gradually becoming an emerging bioreactor due to its huge biomass [1]. The genus *Nicotiana*, in the family *Solanaceae*, comprises around 76 species in 13 sections [2], of which the species *Nicotiana tabacum* accounts for the vast majority of global tobacco production. Bacterial wilt, caused by *Ralstonia solanacearum* species complex, is one of the most damaging diseases affecting the production of *N. tabacum* worldwide. In addition to tobacco, the bacterium *R. solanacearum* threatens many economically important crops [3], such as tomato, eggplant, pepper, and peanut, usually invading plant roots through root tips, secondary root emergence sites, and wounds [4]. After entering plant roots, the bacteria move to the root vasculature, where they multiply in the xylem and subsequently spread into the shoot. The bacteria secrete exopolysaccharides that can block the xylem, causing plant wilting, root and stem necrosis, stunting, and eventually plant death. The disease is not completely

under control, although a number of agricultural measures, chemical pesticides, and biopesticides have been used. Clearly, molecular breeding for resistance to *R. solanacearum* is a more economical and effective strategy, which will require extensive research into the molecular mechanisms underlying bacterial wilt resistance and a broad identification of defense-related genes against *R. solanacearum* infection.

To date, various types of functional genes associated with bacterial wilt resistance have been identified in plants. In *Arabidopsis*, RRS1, which contains the TIR-NBS-LRR (Toll/interleukin-1 receptor, nucleotide binding-site, and leucine-rich repeat) domains and a WRKY (the WRKYGQK heptapeptide) motif, physically interacts with another TIR-type R protein, RPS4, to confer broad-spectrum resistance to several strains of *R. solanacearum*, involving the physical interaction between the RRS1/RPS4 complex and the avirulence type III effector PopP2 [5–8]. The *ERECTA* gene, which encodes a leucine-rich repeat receptor-like kinase, confers disease resistance to *R. solanacearum* and also affects the development of aboveground organs [9]. In pepper, a series of *WRKY* genes have been shown to regulate resistance to *R. solanacearum* infection [10]. The NAC (NAM, ATAF1/2, and CUC2) family is another widely studied transcription factor involved in the regulation of bacterial wilt resistance, including *SmNAC* in eggplant [11], *StNACb4* in potato [12], *SlNAP1* in tomato [13], and *CaNAC2c* and *CaNAC029* in pepper [14]. Other types of transcription factors are also involved, such as the ethylene response factor (ERF) proteins SlERF3 [15] and SlERF5 [16] in tomato, the basic leucine zipper (bZIP) protein CabZIP63 [17] in pepper, the R2R3-MYB (v-myb avian myeloblastosis viral oncogene homolog) protein SmMYB44 [18] in eggplant, and the basic helix–loop–helix (bHLH) protein bHLH93 [19] in *Nicotiana benthamiana*. Additionally, in pepper CaHsfB2a, a nuclear-localized heat shock factor, binds the promoters of both *CaWRKY6* and *CaWRKY40* and positively regulates plant immunity to *R. solanacearum* [20]; CaASR1, an abscisic acid-, stress-, and ripening-inducible protein, physically interacts with CabZIP63 and acts as a positive regulator of the pepper defense response to *R. solanacearum* [21]. In potatoes, StMKK1, a mitogen-activated protein kinase kinase, suppresses pathogen-associated molecular pattern (PAMP)-triggered immunity (PTI) and salicylic acid (SA)-related signaling pathways and thus negatively regulates potato defense against *R. solanacearum* [22]. There are several metabolism-related enzymes that play a significant role in the bacterial wilt defense response, including a spermidine synthase from eggplant [18] and pyruvate decarboxylases from *Arabidopsis* and tomato [23]. In *N. tabacum*, the functional studies of bacterial wilt resistance-related genes have been largely limited and only a few functional genes have been characterized, including the WRKY IIc transcription factor NtWRKY50 [24], the pathogenesis-related protein 3 (PR-3) member NtPR-Q [25], the PR-1 member NtPR1a [26], and the E3 ubiquitin ligase NtRNF217 [27]. It is clear that a broader identification of candidate genes regulating plant immunity to *R. solanacearum* should be carried out in *N. tabacum*.

Comparative transcriptome analysis has great potential to elucidate the molecular mechanisms underlying bacterial wilt resistance and to identify candidate genes for enhancing plant immunity to *R. solanacearum* infection. Gao et al. analyzed the transcriptional response in the seedling roots of D101 (resistant) and CBH (susceptible) at 3 h after inoculation with *R. solanacearum* and proposed that in the tobacco root, glutathione and flavonoids may be the causal agents conferring early resistance to *R. solanacearum* infection [28]. Subsequently, the expression profiles in the rootstalks of Fandi3 (resistant) and Yunyan87 (susceptible) at 1, 3, and 7 days after *R. solanacearum* infection were investigated, and the researchers also demonstrated that glutathione metabolism and phenylpropane metabolism function as primary resistance pathways to *R. solanacearum* infection [29]. In addition, the researchers highlighted *WRKY6*, *WRKY11*, *ERF5*, *ERF15*, and *PR5* for their possible involvement in disease resistance. Pan et al. analyzed the transcriptome changes of the whole stem tissue of 4411-3 (highly resistant) and K326 (moderately resistant) at 0, 10, and 17 days after *R. solanacearum* inoculation and revealed that differentially expressed genes related to cell wall development, starch and sucrose metabolism, glutathione metabolism, ABC transporters, endocytosis, glycerolipid metabolism, and glycerophos-

pholipid metabolism may be involved in plant defense response against *R. solanacearum* infection [30]. Additionally, the researchers proposed that auxin and abscisic acid (ABA) levels, as well as the genes controlling them, play an important role in the interaction between tobacco and *R. solanacearum*. Alariqi et al. performed a large-scale comparative transcriptome analysis of tobacco roots at 0, 12, 24, 36, 48, 72, and 120 h after *R. solanacearum* infection based on Yanyan97 (resistant) and Honghuadajinyuan (susceptible) [31]. In the study, they presented that phytohormones, glutathione, phenylpropanoids, and secondary metabolites are strongly associated with tobacco resistance to bacterial wilt. Although the above studies have, in a sense, investigated the dynamic changes in the tobacco transcriptome under *R. solanacearum* infection, there is still a significant research space in this area, especially the transcriptome landscapes of near-isogenic lines that exhibit distinct resistance to bacterial wilt.

Chromosome segment substitution lines (CSSLs) are valuable genetic resources for basic and applied research on the improvement of complex traits [32]. To elucidate the genetic basis of bacterial wilt resistance, we developed a BC_4F_5 population using the major tobacco cultivar K326 as the recipient and the classic resistant cultivar OX2028 as the donor. Among the BC_4F_5 lines, we identified two lines, C244 and C010, with higher resistance to *R. solanacearum* than the recurrent parent K326, and a more susceptible line, C035. In general, the colonization of host plant roots by *R. solanacearum* involves two phases: the propagation phase, in which the bacteria spread through the cortex via intercellular spaces, and the proliferation phase, in which the bacteria enter the vascular system and begin massive replication [4,33]. Under appropriate conditions, the bacterial colonization of the xylem can be observed as early as 24 h after *R. solanacearum* infection [34,35], encouraging us to focus on the early stages of bacterial invasion. In the present study, we therefore performed a large-scale comparative transcriptome analysis of seedling roots of C244, C010, and C035 at 3, 9, 24, and 48 h after *R. solanacearum* infection. The transcriptome landscape differences between C244, C010, and C035 under *R. solanacearum* infection were revealed and the candidate genes regulating plant immunity against *R. solanacearum* were identified. Our findings will contribute to deciphering molecular mechanisms underlying bacterial wilt resistance and provide alternative genes for molecular breeding to improve bacterial wilt resistance.

2. Materials and Methods

2.1. Plant Materials and Growth Conditions

The BC_4F_5 population used in this study was constructed from tobacco cultivars K326, which is moderately resistant to bacterial wilt, and OX2028, a traditional resistant source. The seeds of K326 and OX2028 (with accession numbers 00002266 and 00003791, respectively) were obtained from the National Tobacco Germplasm Resource Genebank in the Institute of Tobacco, Chinese Academy of Agricultural Sciences, with appropriate permissions. First, K326 as the female parent was crossed with OX2028 to generate the F_1 hybrid in Qingdao, Shandong Province, China, in the summer of 2014. The hybrid plants were then continuously backcrossed with K326 as the recurrent parent for four generations to produce BC_4F_1 plants in Qingdao in the summer of 2015 to 2017 and in Xishuangbanna in the winter of 2017. Finally, the BC_4F_1 plants were self-pollinated for four generations in Qingdao in the summer of 2018 to 2021, producing the BC_4F_5 plants (Figure S1a). To ensure the introgression of OX2028 into K326, molecular marker-assisted selection was performed on generations BC_2F_1 to BC_4F_3.

After identifying the bacterial wilt resistance of BC_4F_5 seedlings, the BC_4F_5 lines C244, C010, and C035 were selected to generate RNA-seq data because C244 and C010 are more resistant to *R. solanacearum* than the recurrent parent K326, but C035 is more susceptible to the bacterium than K326. The sterile seeds of C244, C010, and C035 were planted in germination boxes with nutrient soil in a phytotron (25 °C, 16 h light/8 h dark, and 70% relative humidity), and then the one-month-old seedlings were transferred to 50% Hoagland's solution and changed every five days under the environmental conditions listed

above. When the seedlings grew to the five-leaf stage (about two months old), the seedling roots of the treatment group were inoculated with an *R. solanacearum* strain Y45 [36] isolated from the diseased tobacco plant in Yunnan Province, China, which was resuspended with water to a concentration of 1.0×10^8 cfu/mL. At two hours post inoculation (hpi), the seedling roots were carefully washed with water and subsequently returned to 50% Hoagland's solution. The *R. solanacearum*-inoculated roots were collected independently at 3, 9, 24, and 48 hpi, and three biological replicates were generated at each time point, with each replicate containing at least five individual plants. The collected samples were immediately frozen with liquid nitrogen and then stored at −80 °C. For the control group, seedling roots were inoculated with water instead of *R. solanacearum* suspension, and root samples were also collected at the corresponding time points. Note that the ambient temperature was adjusted to 28 °C one day before inoculation with *R. solanacearum* to ensure colonization of the bacterium.

2.2. Transcriptome Sequencing

The frozen root samples were finely ground using liquid nitrogen, and then the total RNA was isolated using a TIANGEN RNAprep Pure Plant Kit (Beijing, China). For RNA-seq, strand-specific cDNA libraries were prepared using a NEBNext Ultra Directional RNA Library Prep Kit for Illumina (Ipswich, MA, USA) at the Novogene Co., Ltd. (Tianjin, China). As a result, cDNA libraries containing 250–300 bp insert fragments were constructed and RNA-seq was performed using an Illumina NovaSeq 6000 platform (San Diego, CA, USA), generating 150 bp paired-end reads. To obtain clean reads, raw data were processed by removing adapter- or polyN-containing reads and low-quality reads. Subsequently, the clean reads were aligned to the *N. tabacum* K326 reference genome (with the accession number PRJNA376174) [37] using Hisat2 v2.0.5 (Baltimore, MD, USA) [38], and the mapped reads were assembled using StringTie v1.3.3b (Baltimore, MD, USA) [39]. The number of reads mapped to each gene was counted using featureCounts v1.5.0-p3 (Melbourne, VIC, AU) [40] to calculate the FPKM (fragments per kilobase of exon per million mapped fragments) of each gene. Differential expression analysis was performed using DESeq2 (Heidelberg, Germany) [41], and genes with an adjusted p-value ≤ 0.05 (Benjamini–Hochberg method) were identified as differentially expressed. Gene Ontology (GO) enrichment analysis was performed using TBtools v1.120 (Guangzhou, China) [42], and terms with an adjusted p-value ≤ 0.05 (Benjamini–Hochberg method) were considered significantly enriched.

2.3. Genome-Wide Identification of Gene Families

In the present study, seven gene families related to cell wall development were systematically identified at the whole genome level based on the *N. tabacum* K326 reference genome [37]. The seven gene families are cellulose synthase and cellulose synthase-like family (CesA/Csl; PF00535 or PF03552), glycosyl hydrolase family 9 (GH9; PF00759), glycosyl transferase family 8 (GT8; PF01501), laccase family (PF00394, PF07731, and PF07732, simultaneously), pectate lyase-like family (PLL; PF00544), pectin methylesterase family (PME; PF01095), and xyloglucan endotransglucosylase/hydrolase family (XTH; PF00722 and PF06955, simultaneously) (Table S1). We also identified the six major heat shock protein families, namely Hsp20 (PF00011), Hsp40 (PF00226), Hsp60 (PF00118), Hsp70 (PF00012), Hsp90 (PF00183), and Hsp100 (PF02861) (Table S1). For each gene family, seed alignments generated from Pfam [43] were downloaded from InterPro [44], and then the candidate genes were systematically identified using HMMER 3.0 [45]. Conserved features were then confirmed using the Batch Web CD-Search tool in the National Center for Biotechnology Information (NCBI; https://www.ncbi.nlm.nih.gov/, accessed on 12 December 2023).

2.4. Validation of RNA-seq Data and Functional Analysis of Nitab4.5_0007488g0040

To verify the precision of RNA-seq data, real-time quantitative PCR (qRT-PCR) was employed to determine the expression profiles of the selected candidate genes. The total

RNA, a portion of which was utilized to generate RNA-seq data, was retrieved for qRT-PCR. First-strand cDNA was synthesized from the total RNA using the Vazyme HiScript III RT SuperMix for qPCR (Nanjing, China), and then qRT-PCR was conducted on the Roche LightCycler 96 Instrument (Basel, Switzerland) with the Vazyme ChamQ SYBR qPCR Master Mix (Nanjing, China). As an allotetraploid, *N. tabacum* contains subgenomes S and T, derived from the ancestors *Nicotiana sylvestris* and *Nicotiana tomentosiformis*, respectively. Therefore, the 3′ end of the qRT-PCR primers was positioned on regions containing either an SNP or an InDel between the target genes and their highly homologous genes in the other subgenome. This helps to distinguish between the expression of target genes and that of their subgenomic homologs. Relative expression levels were calculated using the $2^{-\Delta\Delta Ct}$ method [46] with the histone H3.3 encoding gene (NCBI Reference Sequence: XM_016638287.1) as an internal control, and a two-tailed *t*-test (*p*-value) performed using the GraphPad Prism software (version 10.0.1; San Diego, CA, USA) was used to determine significantly differential expression.

To investigate the contribution of *Nitab4.5_0007488g0040* to tobacco resistance against bacterial wilt, we examined the expression patterns of *Nitab4.5_0007488g0040* in one susceptible tobacco cultivar, Honghuadajinyuan (HD), and three resistant germplasms, Dixie Bright 101 (DB101), Fandisanhao-bing (FD), and K358, in response to *R. solanacearum* infection. The seeds of HD, DB101, FD, and K358 (with accession numbers 00000540, 00001020, 00001341, and 00003767, respectively) were sourced from the National Tobacco Germplasm Resource Genebank in the Institute of Tobacco, Chinese Academy of Agricultural Sciences. The growth conditions and preparation of *R. solanacearum*- and water-inoculated roots conform to those previously mentioned. Virus-induced gene silencing (VIGS) was applied to further ascertain the role of *Nitab4.5_0007488g0040* in bacterial wilt resistance. The 300-bp *Nitab4.5_0007488g0040* target sequence was cloned and subsequently inserted into the TRV2 vector (NCBI GenBank: AF406991.1) via homologous recombination using the Vazyme ClonExpress UItra One Step Cloning Kit (Nanjing, China). Additionally, the TRV2 vector containing a 300-bp fragment of the green fluorescent protein (GFP) gene was constructed for the control group, and the TRV2 vector containing a 300-bp fragment of the phytoene desaturase (PDS) gene for the report group. The TRV2:*Nitab4.5_0007488g0040*, TRV2:*GFP*, TRV2:*PDS*, and TRV1 (NCBI GenBank: AF406990.1) constructs were transferred into the *Agrobacterium* GV3101 strain separately. TRV1- and TRV2-carrying *Agrobacterium* strains were then co-inoculated into the leaves of four-week-old *N. benthamiana* as described by Senthil-Kumar [47]. After the albino phenotype (photobleaching) occurred in the report group (about two weeks after the *Agrobacterium* inoculation), *Nitab4.5_0007488g0040* expression in *Nitab4.5_0007488g0040*-silenced and control plants was assessed using qRT-PCR, with the elongation factor 1 alpha (EF1α) gene (NCBI GenBank: AY206004.1) as an internal reference, to evaluate *Nitab4.5_0007488g0040* silencing efficiency. Following this, both the control plants and the *Nitab4.5_0007488g0040*-silenced plants were infected with the suspension of *R. solanacearum* Y45 (5.0×10^7 cfu/mL, 10 mL per plant) using the root-drenching method. The wilting percentage was calculated in both groups based on the count of wilting plants. To enhance credibility, VIGS was independently repeated three times, with each group containing a minimum of 15 plants.

3. Results

3.1. Overview of Transcriptome Sequencing

To generate genetic materials for revealing molecular mechanisms underlying bacterial wilt resistance and for molecular breeding to improve bacterial wilt resistance, a CSSL population has been developed using K326 (moderately resistant to bacterial wilt) as the recurrent parent and OX2028 (a traditional resistant resource) as the donor parent (Figure S1a). The CSSL population was planted in a field where tobacco bacterial wilt is prevalent, and then the two lines, C244 and C010, stood out for their extremely excellent resistance. Another line, C035, was also of interest because of its high susceptibility to bacterial wilt. The resistance characteristics of C244, C010, and C035 were further determined by inoculat-

ing their five-leaf-old seedlings with an *R. solanacearum* phylotype IB strain Y45 [36] using the root-drenching method (Figures 1a and S1b,c). As shown, compared with K326, C244 and C010 presented stronger resistance against Y45 infection, while C035 was more susceptible. In addition, the differences in the resistance to Y45 between C244, C010, and C035 were also confirmed using the hydroponic systems (Figure 1b,c). Obviously, comparative transcriptome analysis based on C244, C010, and C035 is a promising strategy to identify bacterial wilt resistance-related genes and to unveil underlying resistance mechanisms.

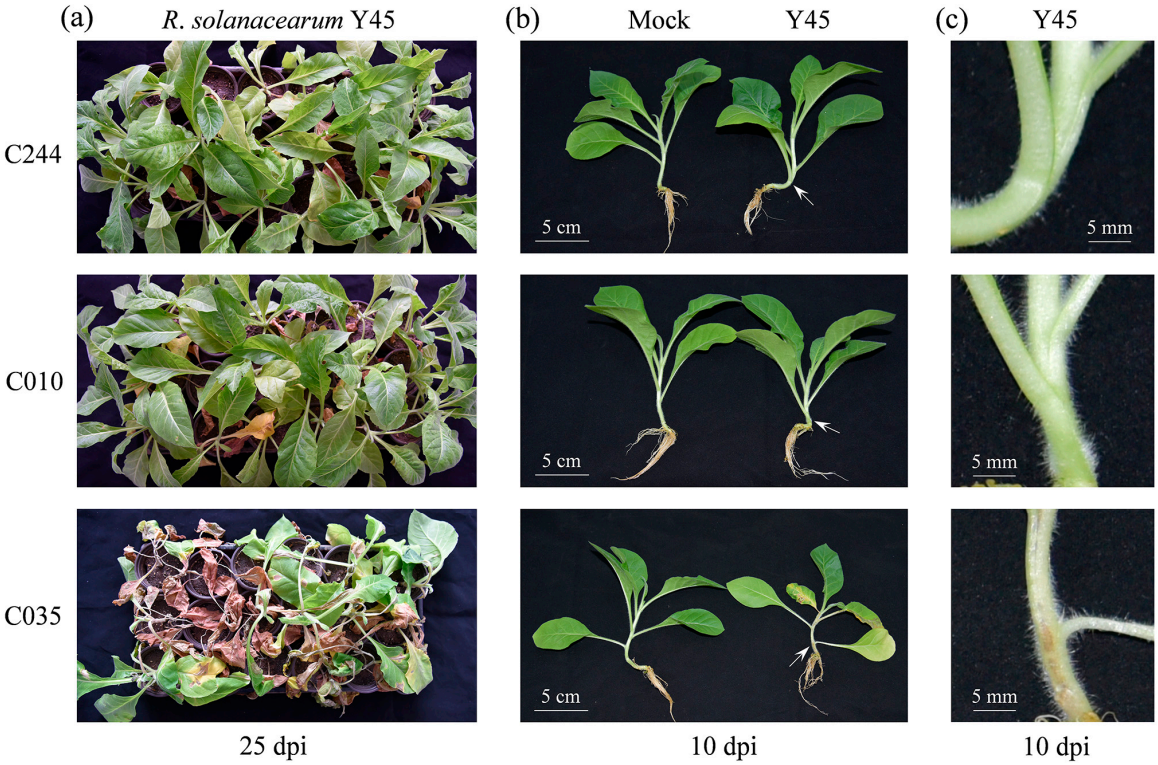

Figure 1. Difference in bacterial wilt resistance between C244, C010, and C035. (**a**) Resistance characteristics under soil culture. (**b**) Resistance characteristics under the hydroponic system. (**c**) Enlarged drawing of the arrow-indicating areas.

To understand the colonization of *R. solanacearum*, we inoculated the roots of five-leaf-old K326 seedlings with a modified Y45 strain carrying a GFP-expressing plasmid (Figure S2). At 3 and 9 hpi, the bacteria had entered the root structure sporadically, whereas at 24 and 48 hpi, the bacteria had massively multiplied in certain root cells. Therefore, we constructed a total of 72 cDNA libraries to perform RNA-seq, generated from the seedling roots of C244, C010, and C035 at 3, 9, 24, and 48 h after inoculation with *R. solanacearum* (indicated as RS) and water (indicated as CK) (Table S2). In summary, 3,077,130,126 RNA-seq clean reads were produced from the 72 cDNA libraries (ranging from 40,215,134 to 47,420,944), accounting for a sum of 461.58 Gb clean bases (ranging from 6.03 Gb to 7.11 Gb), and about 89.90% of the clean reads were mapped to the *N. tabacum* K326 reference genome. Although around 6.57% of the clean reads were mapped to multiple genome locations because of the high homology between the S and T subgenomes, approximately 83.34% were uniquely mapped to the genome for gene expression and differential expression analysis. Clearly, the quantity and quality of the sequencing data are sufficient for further analysis, especially considering that *N. tabacum* is an allotetraploid.

3.2. Early Transcriptional Responses to R. solanacearum Infection

Based on the uniquely mapped clean reads, gene expression analysis was conducted for all the 72 cDNA libraries, and then we carried out principal component analysis (PCA) to display the correlations between the root samples. Analyzed by PC1 (53.7%) and PC2 (22.5%), the three biological replicates in each treatment clustered together, providing further evidence of the accuracy of the RNA-seq workflow (Figure S3). The samples of C244, C010, and C035 at 3 h after inoculation with *R. solanacearum* were closely grouped and clearly separated from the others, showing a significant change in the transcriptional landscape. The other samples were classified by treatment (i.e., *R. solanacearum* vs. water), accessions, and development processes. It seems that the defense responses entered a relatively mild period after the bacteria successfully penetrated the physical barriers. The inference is also supported by the fact that, by comparing the treatment group with the control group, the number of differentially expressed genes (DEGs) at 3 hpi is 5614, 5470, and 6632 in C244, C010, and C035, respectively, whereas it is extremely attenuated at 9, 24, and 48 hpi (Table S3). Specifically, at 3 hpi, 3219, 2837, and 3454 genes were upregulated in C244, C010, and C035, respectively, while 2395, 2633, and 3178 genes were downregulated (Figure 2a). Furthermore, the percentage of commonly upregulated genes accounted for 61.2%, 69.4%, and 57.0% in C244, C010, and C035, respectively, and the percentage of commonly downregulated genes was 53.3%, 48.5%, and 40.2% (Figure 2b,c). Although hundreds of DEGs were uniquely identified and may have contributed to the resistance characteristics, a significant proportion of DEGs was synchronously regulated in C244, C010, and C035 at 3 hpi, in line with the tight clustering of the samples of C244, C010, and C035 at 3 h after inoculation with *R. solanacearum* in PCA.

To uncover the molecular mechanisms underlying the resistance characteristics, we performed Gene Ontology (GO) enrichment analysis to identify significantly enriched biological processes in both the upregulated and downregulated gene sets. As shown, a great number of GO terms were significantly enriched and classified into four categories, i.e., signaling and response (Figure 2d), metabolism (Figure 2e), cell wall (Figure 2f), and development (Figure 2g). As expected, a considerable number of resistance-related processes were enriched in the upregulated gene sets of C244, C010, and C035, including defense response, hormone-mediated signaling pathway, stress-activated protein kinase signaling cascade, glutathione metabolic process, lipid metabolic process, cell wall biogenesis, and xyloglucan metabolic process. Interestingly enough, most of the above-mentioned processes showed a stronger enrichment in C244 and C010, which may have contributed to their high resistance to bacterial wilt. In the case of the downregulated gene sets, the jointly enriched GO terms in C244, C010, and C035 were relatively scarce, in which we highlighted the hydrogen peroxide catabolic process because its enrichment levels in C244, C010, and C035 corresponded to the resistance of C244, C010, and C035, oppositely. A reasonable inference is that the pathogenesis in C035 was more severe and thus called for more ROS levels, supported by the significant upregulation of stress response genes (Figure 2d) and the significant downregulation of development-related genes (Figure 2g) in C035. Additionally, a number of cell wall development-related processes were significantly enriched in the downregulated DEGs of C035, whereas several of them were significantly enriched in the upregulated DEGs of C244 (Figure 2f). Hence, the expression pattern differences of cell wall development-related genes between C244, C010, and C035 might have partly shaped the differences in their resistance characteristics.

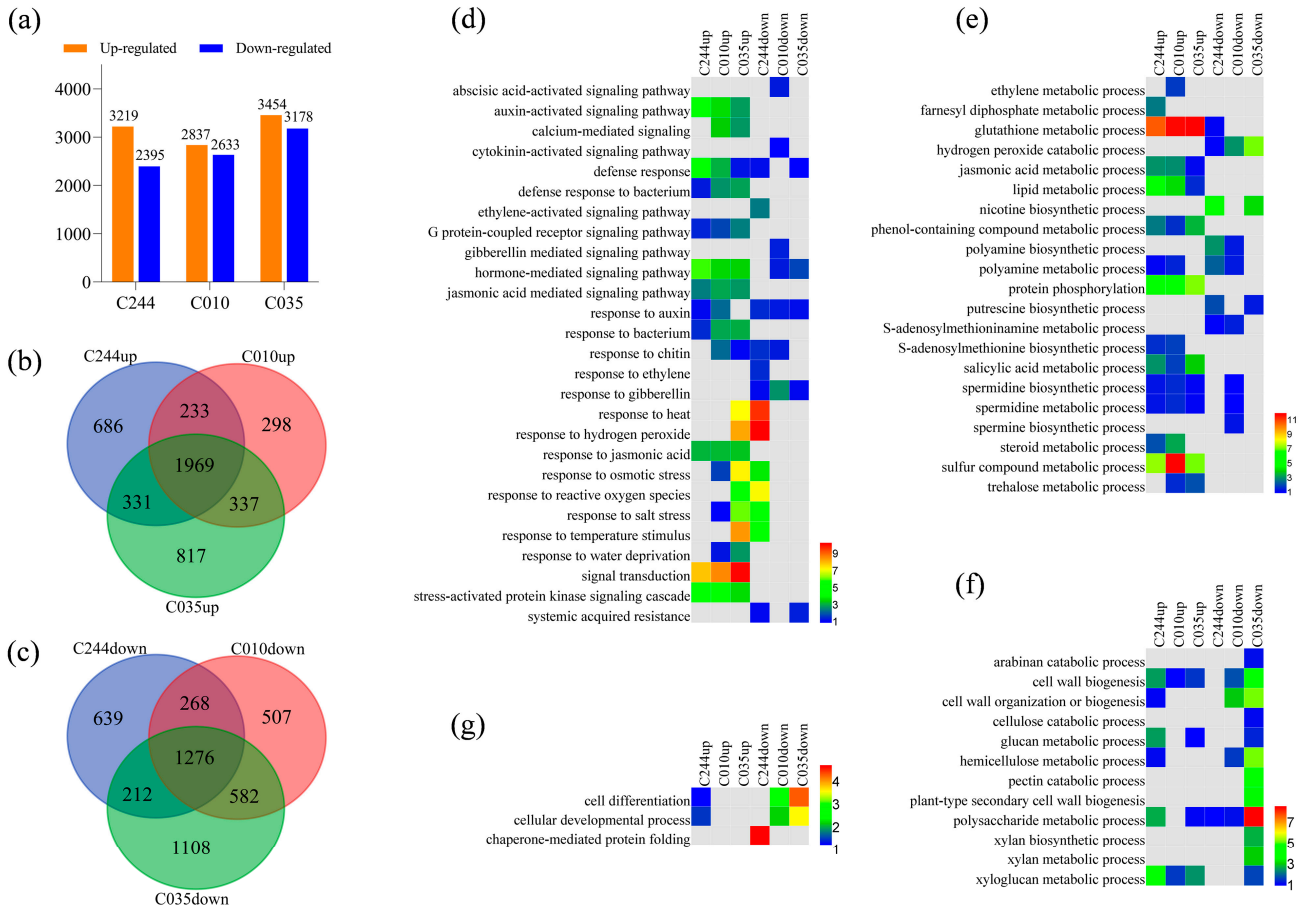

Figure 2. Transcriptional responses to *R. solanacearum* infection at 3 hpi. (**a**) Identification of DEGs at 3 hpi by comparing the treatment group with the control group. (**b**) Venn diagram shows the commonly upregulated genes in C244, C010, and C035 at 3 hpi. (**c**) Venn diagram shows the commonly downregulated genes in C244, C010, and C035 at 3 hpi. GO terms were significantly enriched and artificially classified into four categories, including signaling and response (**d**), metabolism (**e**), cell wall (**f**), and development (**g**). Heatmaps exhibit GO enrichment levels that are calculated as $-\log_{10}{}^{(\text{adjusted } p\text{-value})}$.

3.3. Identification and Expression Analysis of Cell Wall Development-Related Genes

Considering the potential roles of cell wall development-related genes in bacterial wilt resistance, we conducted a genome-wide identification of cellulose synthase and cellulose synthase-like family (CesA/Csl), glycosyl hydrolase family 9 (GH9), glycosyl transferase family 8 (GT8), laccase family, pectate lyase-like family (PLL), pectin methylesterase family (PME), and xyloglucan endotransglucosylase/hydrolase family (XTH), and a total of 86, 53, 90, 92, 47, 156, and 59 members were identified, respectively (Table S4). After the differential expression analysis (treatment vs. control), 21, 13, 27, 33, 13, 33, and 24 members in CesA/Csl, GH9, GT8, laccase, PLL, PME, and XTH, respectively, showed significant expression changes in C244, C010, and C035 at 3 hpi (Figure 3b–h; Table S5). As expected, a number of cell wall development-related genes displayed a stronger upregulation in C244, especially members in GH9, laccase, and PME. On the contrary, members in all these families except GT8 showed a stronger downregulation in C035, even though, as a confusing question, their background expression levels (i.e., expression in the control group) were higher in C035 than in the others. The number of significantly downregulated genes in C010 is between that of C244 and C035 (Figure 3a), consistent with C010's bacterial wilt resistance being intermediate between C244 and C035 (Figure S1c). The results indicate that the early transcriptional responses of cell wall development-related genes may play an

important role in plant immunity against *R. solanacearum*, and the DEGs exhibiting different expression profiles in C244, C010, and C035 could be alternative genes for molecular breeding to improve bacterial wilt resistance.

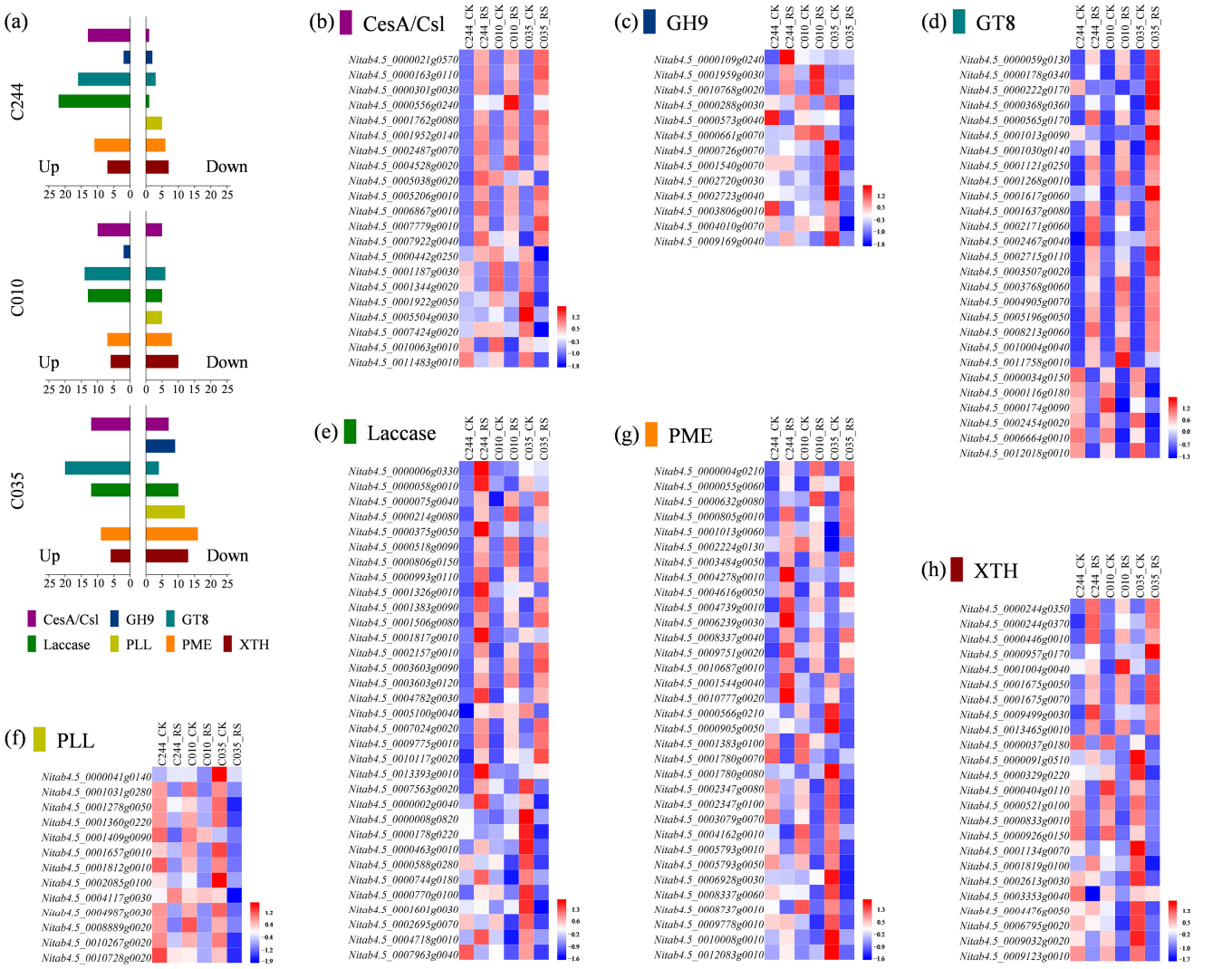

Figure 3. Expression analysis of cell wall development-related genes in response to *R. solanacearum* infection. (**a**) The number of differentially expressed cell wall development-related genes in the different BC_4F_5 lines at 3 hpi. Heatmaps demonstrate expression profiles of cellulose synthase and cellulose synthase-like family (**b**), glycosyl hydrolase family 9 (**c**), glycosyl transferase family 8 (**d**), laccase family (**e**), pectate lyase-like family (**f**), pectin methylesterase family (**g**), and xyloglucan endotransglucosylase/hydrolase family (**h**) in response to *R. solanacearum* infection at 3 hpi. The heatmaps show expression levels normalized using the z-score method. The original FPKM values are available in Table S5.

3.4. Transcriptional Landscape Differences between C244, C010, and C035 in Response to R. solanacearum Infection

At 3 hpi, by comparing the treatment group with the control group, we presented a great change in the transcriptional landscape in C244, C010, and C035 in response to *R. solanacearum* infection, and also highlighted the synchronous and differential regulation of DEGs. In the case of 9, 24, and 48 hpi, the number of DEGs decreased significantly (Table S3). Specifically, at 9 hpi, there were 663, 1540, and 1144 DEGs in C244, C010, and C035, respectively (Figure 4a); at 24 hpi, there were 714, 233, and 719 (Figure 4b); and at 48 hpi, there were 629, 513, and 166 (Figure 4c). However, the GO enrichment analysis

revealed substantial differences between C244, C010, and C035 at 9, 24, and 48 hpi, supported by the percentage of commonly up- or downregulated DEGs in C244, C010, and C035 being extremely low. At 9 hpi, a lot of biological processes were significantly enriched and manually classified into different categories, including protein metabolic process (Figure 4d), signaling and response (Figure 4e), cell wall (Figure 4f), and metabolism (Figure 4g). As shown, a series of processes related to protein folding (Figure 4d) and stress response (Figure 4e) were significantly enriched in the downregulated gene sets of C244, C010, and C035, which was further proven to be mainly due to the significant downregulation of heat shock protein (Hsp) genes. This might be a strategy employed by the bacterium to help in colonization. Hence, it is noteworthy to mention that several protein quality control processes, particularly those in the endoplasmic reticulum (ER), were significantly enriched in the upregulated DEGs of C244, but not C010 and C035 (Figure 4d). Interestingly, the hydrogen peroxide catabolic process was significantly enriched in the downregulated DEGs of C244 and C010, but not C035 (Figure 4g), which might have elevated the ROS levels of C244 and C010 and thus contributed to their bacterial wilt resistance. Similarly, the lignin catabolic process and pectin catabolic process were significantly enriched in the downregulated DEGs of the resistant lines (Figure 4f), which might also be partly responsible for their resistance characteristics. At 24 and 48 hpi, a noticeable observation is the significant enrichment of processes associated with protein folding and stress response in the upregulated DEGs of C244 and C035 (Figure 4h,i), which were significantly enriched in the downregulated DEGs at 9 hpi, indicating a complex interaction between tobacco and *R. solanacearum*. Besides that, at 48 hpi, numerous biological processes concerned with plant immunity including defense response, ethylene metabolic process, jasmonic acid mediated signaling pathway, isoprenoid metabolic process, and steroid metabolic process were significantly enriched in the upregulated DEGs of C244 and C010 (Figure 4i). It appears that C244 partly incorporates the defense mechanisms of C010 and C035, corresponding to its highest resistance to bacterial wilt among the three lines (Figure S1c).

In the analysis above, a series of processes associated with protein quality control and stress response were shown to be mainly involved in heat shock proteins (Hsps). Considering Hsps participate in protein folding, assembly, translocation, and degradation [48], we performed a genome-wide identification of six major Hsp families, namely Hsp20, Hsp40, Hsp60, Hsp70, Hsp90, and Hsp100, and identified a total of 82, 192, 60, 70, 20, and 16 members, respectively (Table S6). Subsequently, a lot of differentially expressed *Hsp* genes were identified by comparing the treatment group with the control group (Figure 5; Tables S7–S12). As anticipated, at 3 hpi, a number of *Hsp* genes, specifically those belonging to the Hsp20, Hsp70, and Hsp100 families, showed significant upregulation in C035 but not in C244 and C010, suggesting a higher level of stress in C035. At 9 hpi, some members from the Hsp20, Hsp70, and Hsp100 families were significantly downregulated in C244, C010, and C035, which might be a strategy of the bacterium to destroy plant defense responses. On the contrary, several *Hsp70* genes were significantly upregulated only in C244, potentially enhancing its resistance to bacterial wilt. Similarly, a few *Hsp70* genes were also significantly upregulated at 24 and 48 hpi in C244, further showing the crucial roles of *Hsp70* in resistance characteristics. Besides that, at 24 and 48 hpi, C244 and C035 demonstrated a higher number of upregulated *Hsp20* genes compared to C010, corresponding to the stronger enrichment of protein folding and stress response processes (Figure 4h,i). The findings indicate that Hsps could have a pivotal function in regulating resistance to bacterial wilt. As such, genetically modifying the *Hsp* genes in response to *R. solanacearum* infection might represent an efficacious approach to improving resistance.

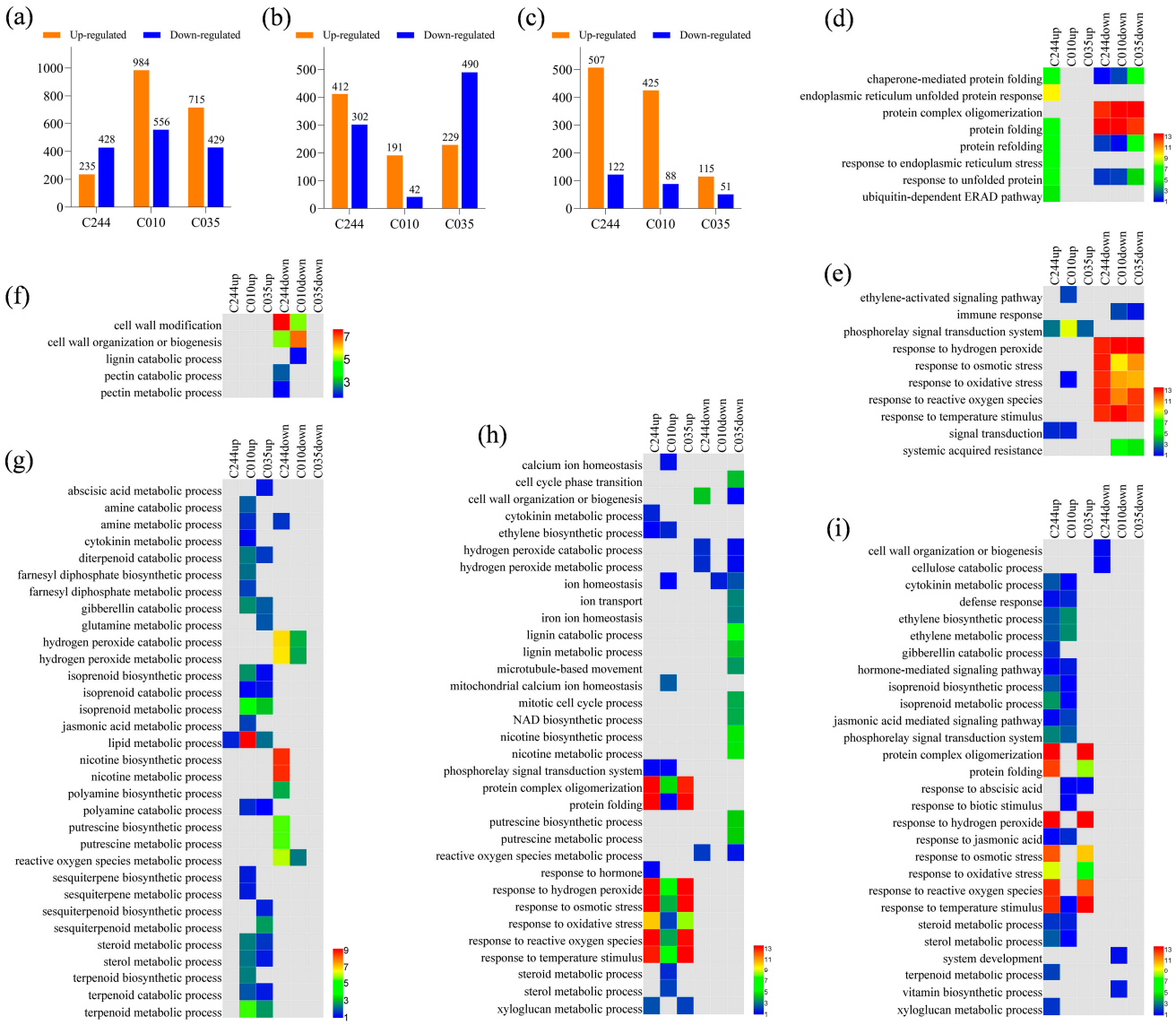

Figure 4. Transcriptional responses to *R. solanacearum* infection at 9, 24, and 48 hpi. (**a**) Identification of DEGs at 9 hpi by comparing the treatment group with the control group. (**b**) Identification of DEGs at 24 hpi. (**c**) Identification of DEGs at 48 hpi. A lot of GO terms were significantly enriched at 9 hpi and manually classified into different categories, including protein metabolic process (**d**), signaling and response (**e**), cell wall (**f**), and metabolism (**g**). (**h**) The significantly enriched GO terms at 24 hpi. (**i**) The significantly enriched GO terms at 48 hpi. Heatmaps exhibit GO enrichment levels that are calculated as $-\log_{10}$(adjusted *p*-value).

3.5. Comparative Transcriptome Analysis Identifies Candidate Genes for Improving Bacterial Wilt Resistance

By comparing the treatment group with the control group, we have presented the differences in transcriptome landscape in response to *R. solanacearum* infection between C244, C010, and C035. To further identify potential genes for enhancing resistance to bacterial wilt, we also conducted a comparative transcriptome analysis of *R. solanacearum*-inoculated root samples from C244 and C035 (Figure 6a; Table S3), as well as C010 and C035 (Figure 6c; Table S3). As a consequence, a number of genes related to protein folding and stress response showed higher expression levels in C035 than in C010 at 3, 24, and 48 hpi (Figure 6d). For C244 vs. C035, these types of genes possessed higher expression at 3 hpi but lower expression at 9 and 24 hpi in C035 (Figure 6b). Clearly, it is improbable that the superior resistance of C010 as compared to C035 can be attributed to protein folding and

stress response mechanisms. Subsequently, 34 and 67 genes were refined whose expression was consistently higher in C244 and C010, respectively, compared with C035 (Figure 6e,f). It is extremely interesting that 33 genes were shared, given that only a few dozen genes were utilized (Figure 6g). Among the 33 DEGs, some have been shown to be closely associated with plant disease resistance, including GRAS transcription factor [49], calcium-binding protein [50], alternative oxidase [51], receptor-like protein [52], universal stress protein [53], C2H2-type zinc finger protein [54], and pathogenesis-related protein 1 [26] (Table S13).

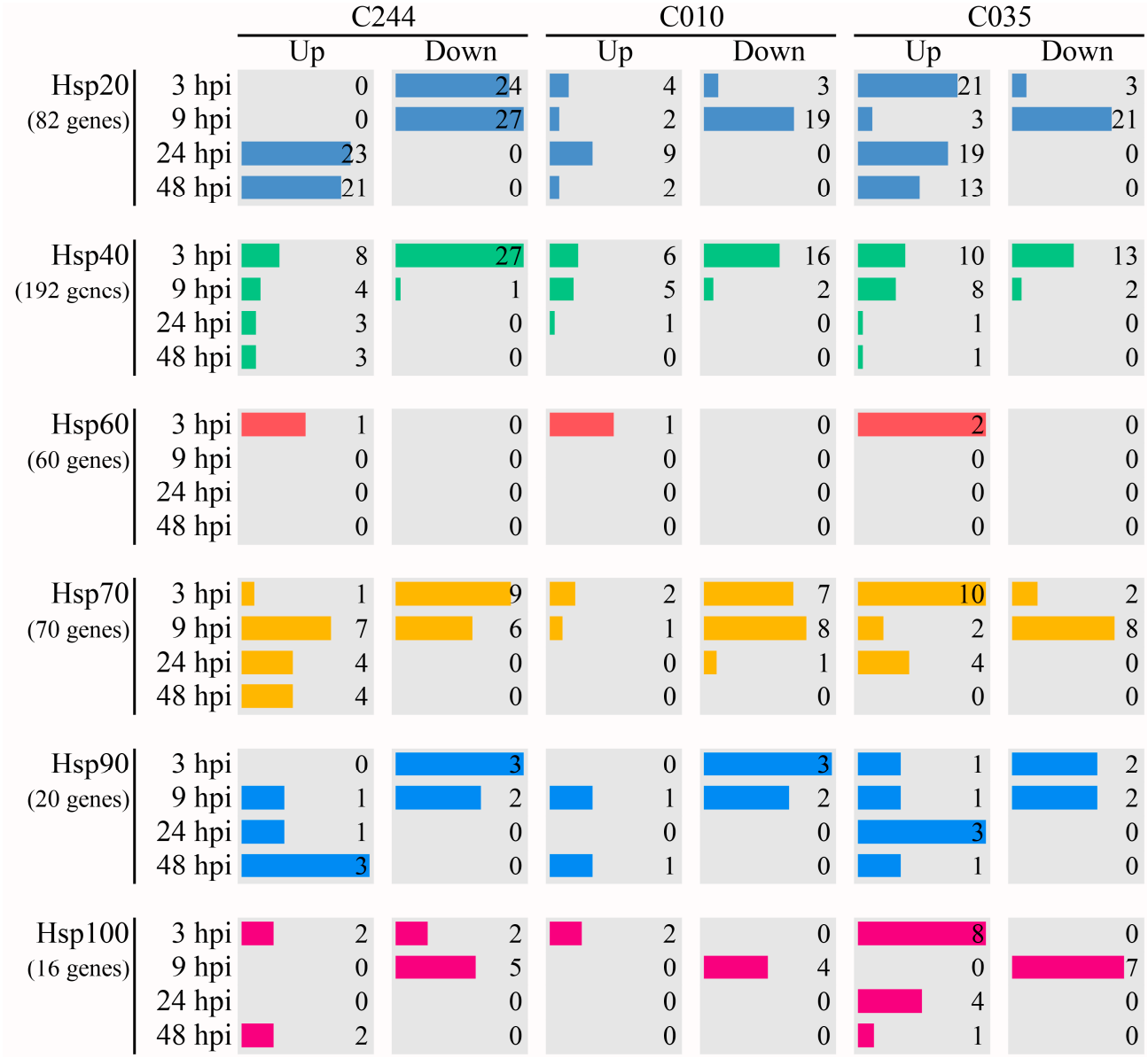

Figure 5. Identification of differentially expressed *Hsp* genes in response to *R. solanacearum* infection. The leftmost numbers represent the number of *Hsp* genes in the *N. tabacum* K326 reference genome. The numbers in the panels represent the number of differentially expressed *Hsp* genes in response to *R. solanacearum* infection. The detailed gene identifiers are available in Tables S6–S11. FPKM values of *Hsp* genes in response to *R. solanacearum* and water are available in Table S12.

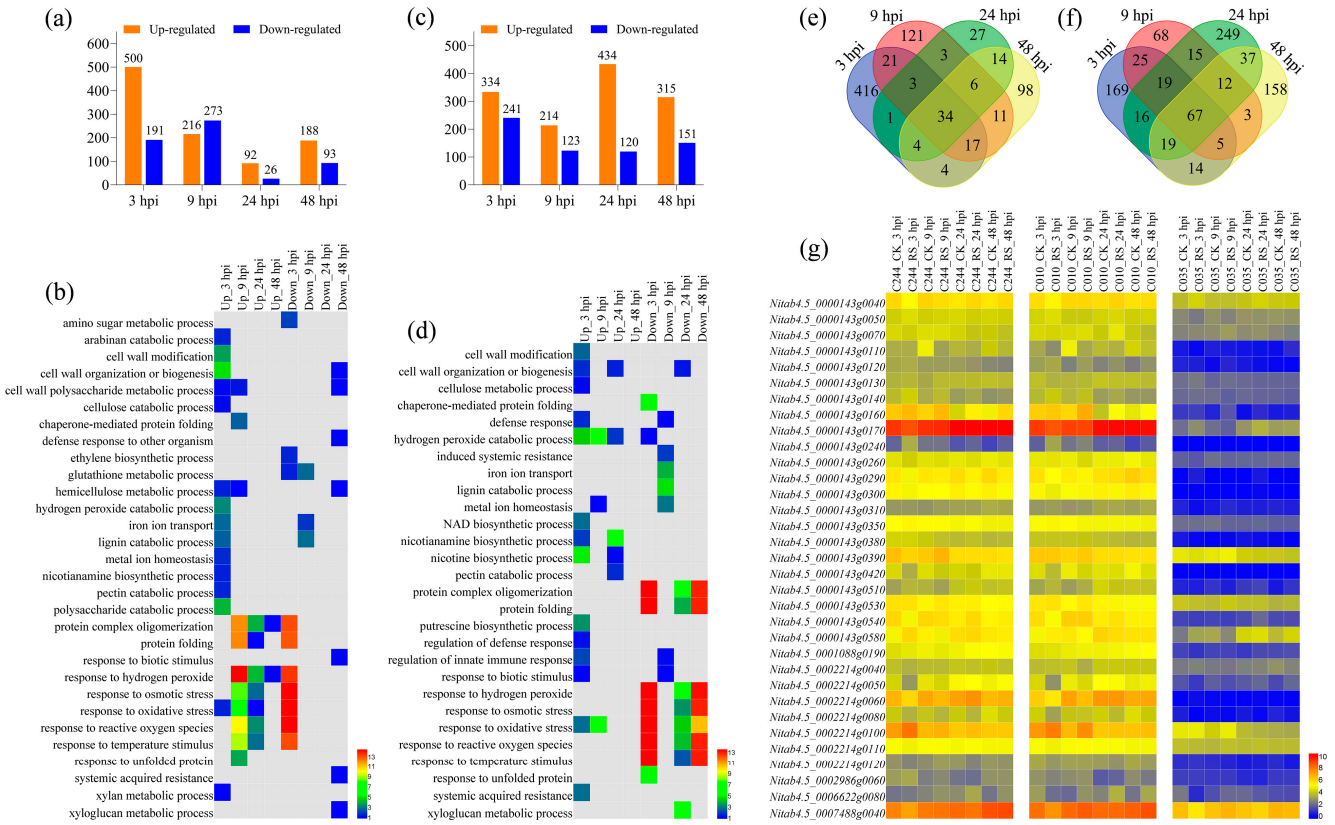

Figure 6. Comparative transcriptome analysis of *R. solanacearum*-inoculated root samples from C244 and C035, as well as C010 and C035. (**a**) Identification of DEGs in C244 versus C035. (**b**) The significantly enriched GO terms in C244 versus C035. Heatmap exhibits GO enrichment levels that are calculated as $-\log_{10}{}^{(\text{adjusted } p\text{-value})}$. (**c**) Identification of DEGs in C010 versus C035. (**d**) The significantly enriched GO terms in C010 versus C035. (**e**) Venn diagram shows the commonly upregulated genes at 3, 9, 24, and 48 hpi in C244 versus C035. (**f**) Venn diagram shows the commonly upregulated genes at 3, 9, 24, and 48 hpi in C010 versus C035. (**g**) Expression profiling of the 33 candidate genes. Heatmap exhibits gene expression levels that are calculated as $\log_2{}^{(1+\text{FPKM})}$.

To verify the expression profiles of the candidate genes, we selected four genes, namely *Nitab4.5_0000143g0170*, *Nitab4.5_0000143g0290*, *Nitab4.5_0002214g0060*, and *Nitab4.5_0007488g0040*, for qRT-PCR analysis, taking into account their expression levels and functional annotation (Figure 6g; Table S13). Gene-specific primers were developed (Table S14) and a lower expression of the four genes in C035 compared to C244 and C010 was observed (Figure 7a). As a member of the pathogenesis-related protein 1 (PR-1) family, *Nitab4.5_0007488g0040* potentially has a crucial function in plant defense mechanisms, which motivates us to investigate its expression patterns within cultivars with varying resistance to bacterial wilt (Figure 7b). As shown, *Nitab4.5_0007488g0040* exhibited higher expression levels in the root tissue of the three resistant germplasms (DB101, FD, and K358) in comparison to the susceptible cultivar HD. To further confirm the involvement of *Nitab4.5_0007488g0040* in plant immunity against *R. solanacearum*, virus-induced gene silencing (VIGS) was utilized for silencing the homologs of *Nitab4.5_0007488g0040* in *N. benthamiana*. After the albino phenotype occurred in the report group (Figure 7c), the significantly lower expression of the homologs of *Nitab4.5_0007488g0040* was observed in *Nitab4.5_0007488g0040*-silenced plants compared with the control plants (Figure 7d; Table S14). As expected, *Nitab4.5_0007488g0040*-silenced plants, compared with the control plants, showed more susceptibility to *R. solanacearum* infection (Figures 7e,f and S4). The results suggest that *Nitab4.5_0007488g0040* positively regulates tobacco defense response against *R. solanacearum* infection and should be an important resource to improve bacterial wilt resistance.

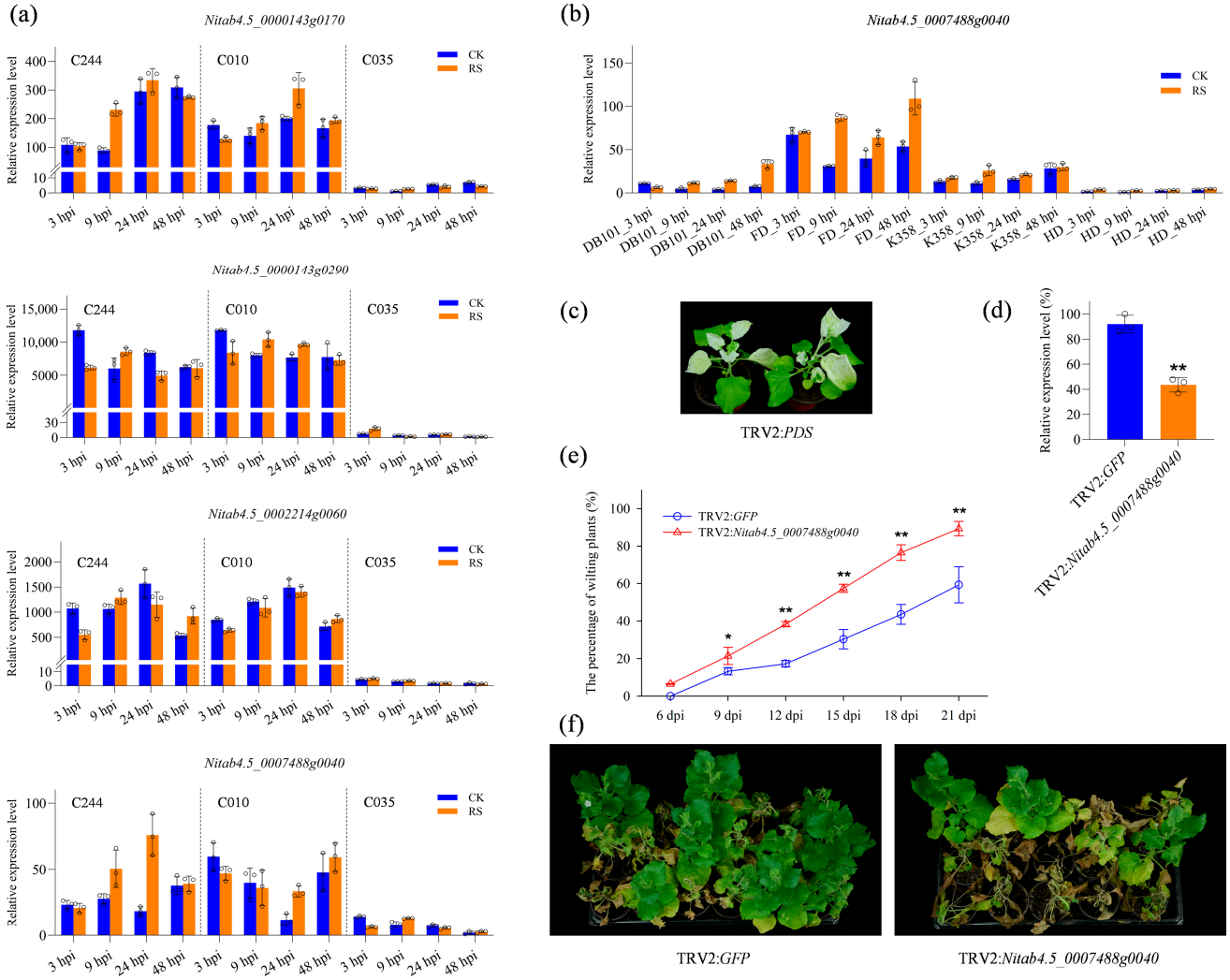

Figure 7. Functional analysis of *Nitab4.5_0007488g0040*. (**a**) Validation of the expression patterns of selected candidate genes via qRT-PCR. (**b**) The expression patterns of *Nitab4.5_0007488g0040* within germplasms with varying resistance to bacterial wilt. (**c**) The albino phenotype of TRV2:*PDS* plants. (**d**) Silencing of the homologs of *Nitab4.5_0007488g0040* in *N. benthamiana*. (**e**) The wilting percentage of TRV2:*GFP* and TRV2:*Nitab4.5_0007488g0040* plants. (**f**) Disease symptoms of TRV2:*GFP* and TRV2:*Nitab4.5_0007488g0040* plants inoculated with Y45 by root irrigation at 21 dpi. Bars represent the mean ± standard deviation. Data were analyzed using a two-tailed *t*-test and asterisks indicate statistically significant differences (* $p < 0.05$ and ** $p < 0.01$).

4. Discussion

Comparative transcriptome analysis between tobacco germplasms with different resistance to bacterial wilt is an effective strategy to elucidate resistance mechanisms and identify candidate genes for marker-assisted selection or genetic modification to improve bacterial wilt resistance. For this purpose, a large-scale comparison of transcriptome landscapes in response to *R. solanacearum* infection has been performed between tobacco cultivars with differences in bacterial wilt resistance as well as botanical characteristics [28,29,31]. By comparison, in the current study, three CSSLs (namely BC_4F_5 lines) with varying bacterial wilt resistance were utilized to carry out comparative transcriptome analysis, which may contribute to a much easier understanding of molecular mechanisms underlying bacterial wilt resistance. Similarly, Pan et al. compared the bacterial wilt defense-related transcriptomes of two tobacco materials, K326 and a K326-derived BC_4F_5 line 4411-3, but the work focused on the whole stem tissue at 0, 10, and 17 days after *R. solanacearum* inoculation [30].

In the aforementioned studies, processes regarding glutathione and phenylpropanoid metabolisms have been identified as key resistance pathways to *R. solanacearum* infection [28–31]. In our study, the glutathione metabolic process also emerges as one of the most significantly enriched pathways in early transcriptional responses to *R. solanacearum* infection (Figure 2). Besides that, the hormone-mediated signaling pathway and stress-activated protein kinase signaling cascade stand out in the present study, showing that signal transduction plays a vital role in regulating tobacco immunity against bacterial wilt. In the hormone-mediated signaling pathway, in addition to the signaling pathways of the established defense-associated plant hormones, salicylic acid (SA) and jasmonic acid (JA), the significance of auxin signaling is emphasized (Figure 2). There is growing evidence that auxin plays multiple roles during plant–pathogen interactions [55,56]. In general, auxin signaling results in the activation of defenses for inhibiting the disease of some necrotrophic pathogens, but promotes the disease of some biotrophic pathogens through SA-dependent and/or SA-independent mechanisms. Hence, it is possible that auxin could play a significant role in the interaction between tobacco and *R. solanacearum*. The inference is supported by the observation that the high resistance of GDSY (sun-cured tobacco) to bacterial wilt is attributed to the single amino acid mutation of an auxin transporter-like protein (acc. CN202110841145, China National Intellectual Property Administration). Further genetic experiments are required to accurately confirm the role of auxin in bacterial wilt resistance, either positive or negative.

The plant cell wall not only provides mechanical support essential for growth and development but also acts as a physical and defensive barrier against pathogens. For this reason, pathogens usually secrete cell wall degrading enzymes, such as cellulase, pectinase, xylanase, and xyloglucanase, to penetrate cell wall defenses and cause infections [57]. Then, this can activate the cell wall integrity (CWI) maintenance mechanism by the recognition of damage-associated molecular patterns (DAMPs) or the sensing of changes in the status of the cell wall–plasma membrane continuum to trigger plant disease resistance responses [58,59]. In this study, we highlighted the potential roles of cell wall development-related processes in bacterial wilt resistance and carried out a genome-wide identification of CesA/Csl, GH9, GT8, laccase, PLL, PME, and XTH families. These gene families were selected for their involvement in the synthesis and/or remodeling of cellulose (CesA/Csl and GH9), hemicellulose (CesA/Csl, GH9, and XTH), pectin (GT8, PLL, and PME), and lignin (laccase), which are the main macromolecules of the plant cell wall [60,61]. We then identified a set of family members that showed significant expression changes in response to *R. solanacearum* infection and proposed those whose expression patterns showed significant differences between C244, C010, and C035 as candidate genes for improving bacterial wilt resistance (Figure 3). In a variety of plants, the deposition of cellulose and lignin usually shows increased resistance to pathogenic bacteria, whereas the plot becomes more complicated in the case of hemicellulose and pectin, partly because of the extensive modification of acetylation or methylation [62]. Therefore, the genetic characteristics of the cell wall development-related candidate genes in bacterial wilt resistance should be further confirmed before using them for molecular breeding.

Throughout this study, we have shown that the processes associated with protein quality control and stress response are potentially involved in tobacco defense against *R. solanacearum* infection. Intriguingly, these processes were further found to be mainly supported by heat shock proteins. As a result, we systematically identified members from the major Hsp families, grouped by their molecular weight in kilo Dalton (kDa), including Hsp20, Hsp40, Hsp60, Hsp70, Hsp90, and Hsp100 [48,63], at the genome-wide level. Subsequently, we identified and counted the *Hsp* genes that were significantly differentially expressed in response to *R. solanacearum* infection (Figure 5; Tables S6–S12). Hsp60 proteins have an essential role in de novo protein folding and assembly, as well as refolding stress-denatured proteins [64]. In *Lactuca sativa*, seven out of 22 *Hsp60* genes were significantly differentially expressed in response to UV and high-intensity light stress [65]; in *Sorghum bicolor*, several of the 36 *Hsp60* genes showed abiotic stress-induced expression

patterns [66]. However, our study suggests that *Hsp60* genes are inactive in seedling roots in response to *R. solanacearum* infection, as only two out of 60 *Hsp60* genes were significantly induced. Instead, *Hsp20* and *Hsp70* genes were extensively and dynamically regulated, with some genes displaying distinct expression patterns between C244, C010, and C035. As ATP-independent molecular chaperones, Hsp20 functions in preventing protein degradation, maintaining protein functional conformation, and the refolding of denatured proteins [67]. In association with various cofactors, Hsp70 performs diverse functions using the energy of ATP hydrolysis, including protein folding, translocation across organelle membranes, and disaggregation of aggregates [64]. Although complex and elusive, heat shock proteins are increasingly receiving attention in the field of plant–microbiome interactions [48,63,67,68]. Therefore, the genetic manipulation of *Hsp* genes to enhance protein quality control and stress response should be a novel alternative way to improve bacterial wilt resistance.

In addition to revealing transcriptome landscape changes in response to *R. solanacearum* infection, we have also identified genes with differential expression between *R. solanacearum*-inoculated root samples from C244 and C035, as well as C010 and C035, regardless of whether these genes respond to *R. solanacearum* infection (Figure 6). This strategy holds significant potential in identifying not only *R. solanacearum*-induced defense genes but also those with constitutive expression, considering that C244, C010, and C035 have similar genetic backgrounds but different bacterial wilt resistance. As a result, 33 candidate genes were highlighted for their consistently higher expression in C244 and C010 than in C035, of which some have great potential in modulating plant disease resistance [26,49–54]. Among them, *Nitab4.5_0007488g0040*, encoding a PR-1 protein, was then suggested to positively regulate bacterial wilt resistance, supported by qRT-PCR within cultivars with varying resistance to bacterial wilt and VIGS in *N. benthamiana* (Figure 7). Although the precise mode of action has remained elusive, plant PR-1 proteins play a pivotal role in immune defense, possibly through potent antimicrobial activity, the release of a C-terminal CAPE1 peptide to activate an immune response, and/or recruitment of other PR proteins including thaumatin-like proteins (PR5) and lipid transfer proteins (PR14) [69]. Liu et al. showed that the overexpression of *NtPR1a* contributes to improved resistance to *R. solanacearum* in *N. tabacum* by activating defense-related genes [26]. However, the fact that *Nitab4.5_0007488g0040* differs significantly from *NtPR1a* in nucleotide sequences suggests *Nitab4.5_0007488g0040* as an alternative gene resource for improving bacterial wilt resistance.

5. Conclusions

In the present study, we highlighted a batch of biological processes that were differentially enriched between C244, C010, and C035, and thus further revealed the genetic basis underlying bacterial wilt resistance. In combination with genome-wide gene family identification, we emphasized a number of cell wall development-related genes and *Hsp* genes with great potential in modulating tobacco disease resistance. By comparative transcriptome analysis, we identified a further 33 bacterial wilt resistance-related candidate genes, whose potential roles were then confirmed by qRT-PCR and VIGS assays. These findings not only provide valuable information for the understanding of bacterial wilt resistance but also contribute credibly to tobacco biological breeding for resistance improvement.

Supplementary Materials: The following supporting information can be downloaded at: https://www.mdpi.com/article/10.3390/agronomy14020250/s1, Figure S1: Difference in bacterial wilt resistance between C244, C010, K326, and C035; Figure S2: Fluorescence microscopy of the tobacco roots inoculated with *GFP*-tagged *Ralstonia solanacearum*; Figure S3: Principal component analysis of the sequencing samples based on gene expression; Figure S4: Disease symptoms of TRV2:*GFP* and TRV2:*Nitab4.5_0007488g0040* plants inoculated with Y45 by root irrigation at 21 dpi; Table S1: Conserved features used to perform genome-wide identification of gene families in this study; Table S2: Statistics on RNA-seq data; Table S3: List of DEGs identified in this study; Table S4: List of cell wall biosynthesis-related genes identified in *N. tabacum* in the current study; Table S5: FPKM values of cell wall development-related genes in response to *R. solanacearum* and water in this study; Table S6: List of heat shock proteins (Hsps) identified in *N. tabacum* in the

current study; Table S7: Differentially expressed *Hsp20* genes in response to *R. solanacearum* infection; Table S8: Differentially expressed *Hsp40* genes in response to *R. solanacearum* infection; Table S9: Differentially expressed *Hsp70* genes in response to *R. solanacearum* infection; Table S10: Differentially expressed *Hsp90* genes in response to *R. solanacearum* infection; Table S11: Differentially expressed *Hsp100* genes in response to *R. solanacearum* infection; Table S12: FPKM values of *Hsp* genes in response to *R. solanacearum* and water in this study; Table S13: DEGs with consistently higher expression in C244 and C010 as compared with C035; Table S14: Primer sequences used in this study.

Author Contributions: Conceptualization, L.C. and A.Y.; methodology, Z.L. and Z.X.; software, M.R., H.X. and G.B.; validation, Z.L. and H.Z.; formal analysis, Z.L.; investigation, R.G., X.W. and H.Z.; resources, D.L. and C.J.; data curation, Z.L. and Z.X.; writing—original draft preparation, Z.L.; writing—review and editing, L.C. and A.Y.; visualization, Z.L.; supervision, A.Y.; project administration, L.C.; funding acquisition, L.C. and A.Y. All authors have read and agreed to the published version of the manuscript.

Funding: This research was funded by the Agricultural Science and Technology Innovation Program of CAAS (ASTIP-TRIC01).

Data Availability Statement: The data that support the findings of this study are included in this published article and its additional files. The RNA-seq data are available in the Genome Sequence Archive in the National Genomics Data Center, China National Center for Bioinformation (https://ngdc.cncb.ac.cn/gsa/, accessed on 12 December 2023; accession number: CRA013874) or from the corresponding author upon reasonable request.

Conflicts of Interest: The authors declare no conflicts of interest.

References

1. Molina-Hidalgo, F.J.; Vazquez-Vilar, M.; D'Andrea, L.; Demurtas, O.C.; Fraser, P.; Giuliano, G.; Bock, R.; Orzaez, D.; Goossens, A. Engineering metabolism in *Nicotiana* species: A promising future. *Trends Biotechnol.* **2021**, *39*, 901–913. [CrossRef] [PubMed]
2. Knapp, S.; Chase, M.W.; Clarkson, J.J. Nomenclatural changes and a new sectional classification in *Nicotiana* (Solanaceae). *Taxon* **2004**, *53*, 73–82. [CrossRef]
3. Jiang, G.; Wei, Z.; Xu, J.; Chen, H.; Zhang, Y.; She, X.; Macho, A.P.; Ding, W.; Liao, B. Bacterial wilt in China: History, current status, and future perspectives. *Front. Plant Sci.* **2017**, *8*, 1549. [CrossRef] [PubMed]
4. Xue, H.; Lozano-Duran, R.; Macho, A.P. Insights into the root invasion by the plant pathogenic bacterium *Ralstonia solanacearum*. *Plants* **2020**, *9*, 516. [CrossRef] [PubMed]
5. Deslandes, L.; Olivier, J.; Theulieres, F.; Hirsch, J.; Feng, D.X.; Bittner-Eddy, P.; Beynon, J.; Marco, Y. Resistance to *Ralstonia solanacearum* in *Arabidopsis thaliana* is conferred by the recessive *RRS1-R* gene, a member of a novel family of resistance genes. *Proc. Natl. Acad. Sci. USA* **2002**, *99*, 2404–2409. [CrossRef] [PubMed]
6. Deslandes, L.; Olivier, J.; Peeters, N.; Feng, D.X.; Khounlotham, M.; Boucher, C.; Somssich, I.; Genin, S.; Marco, Y. Physical interaction between RRS1-R, a protein conferring resistance to bacterial wilt, and PopP2, a type III effector targeted to the plant nucleus. *Proc. Natl. Acad. Sci. USA* **2003**, *100*, 8024–8029. [CrossRef] [PubMed]
7. Narusaka, M.; Shirasu, K.; Noutoshi, Y.; Kubo, Y.; Shiraishi, T.; Iwabuchi, M.; Narusaka, Y. *RRS1* and *RPS4* provide a dual *Resistance*-gene system against fungal and bacterial pathogens. *Plant J.* **2009**, *60*, 218–226. [CrossRef]
8. Williams, S.J.; Sohn, K.H.; Wan, L.; Bernoux, M.; Sarris, P.F.; Segonzac, C.; Ve, T.; Ma, Y.; Saucet, S.B.; Ericsson, D.J.; et al. Structural basis for assembly and function of a heterodimeric plant immune receptor. *Science* **2014**, *344*, 299–303. [CrossRef]
9. Godiard, L.; Sauviac, L.; Torii, K.U.; Grenon, O.; Mangin, B.; Grimsley, N.H.; Marco, Y. ERECTA, an LRR receptor-like kinase protein controlling development pleiotropically affects resistance to bacterial wilt. *Plant J.* **2003**, *36*, 353–365. [CrossRef]
10. Hussain, A.; Noman, A.; Khan, M.I.; Zaynab, M.; Aqeel, M.; Anwar, M.; Ashraf, M.F.; Liu, Z.; Raza, A.; Mahpara, S.; et al. Molecular regulation of pepper innate immunity and stress tolerance: An overview of WRKY TFs. *Microb. Pathog.* **2019**, *135*, 103610. [CrossRef]
11. Na, C.; Shuanghua, W.; Jinglong, F.; Bihao, C.; Jianjun, L.; Changming, C.; Jin, J. Overexpression of the eggplant (*Solanum melongena*) NAC family transcription factor *SmNAC* suppresses resistance to bacterial wilt. *Sci. Rep.* **2016**, *6*, 31568. [CrossRef] [PubMed]
12. Chang, Y.; Yu, R.; Feng, J.; Chen, H.; Eri, H.; Gao, G. NAC transcription factor involves in regulating bacterial wilt resistance in potato. *Funct. Plant Biol.* **2020**, *47*, 925–936. [CrossRef] [PubMed]
13. Wang, J.; Zheng, C.; Shao, X.; Hu, Z.; Li, J.; Wang, P.; Wang, A.; Yu, J.; Shi, K. Transcriptomic and genetic approaches reveal an essential role of the NAC transcription factor SlNAP1 in the growth and defense response of tomato. *Hortic. Res.* **2020**, *7*, 209. [CrossRef]

14. Cai, W.; Yang, S.; Wu, R.; Cao, J.; Shen, L.; Guan, D.; Shuilin, H. Pepper NAC-type transcription factor NAC2c balances the trade-off between growth and defense responses. *Plant Physiol.* **2021**, *186*, 2169–2189. [CrossRef] [PubMed]
15. Pan, I.C.; Li, C.W.; Su, R.C.; Cheng, C.P.; Lin, C.S.; Chan, M.T. Ectopic expression of an EAR motif deletion mutant of *SlERF3* enhances tolerance to salt stress and *Ralstonia solanacearum* in tomato. *Planta* **2010**, *232*, 1075–1086. [CrossRef] [PubMed]
16. Li, C.W.; Su, R.C.; Cheng, C.P.; Sanjaya; You, S.J.; Hsieh, T.H.; Chao, T.C.; Chan, M.T. Tomato RAV transcription factor is a pivotal modulator involved in the AP2/EREBP-mediated defense pathway. *Plant Physiol.* **2011**, *156*, 213–227. [CrossRef]
17. Shen, L.; Liu, Z.; Yang, S.; Yang, T.; Liang, J.; Wen, J.; Liu, Y.; Li, J.; Shi, L.; Tang, Q.; et al. Pepper CabZIP63 acts as a positive regulator during *Ralstonia solanacearum* or high temperature-high humidity challenge in a positive feedback loop with CaWRKY40. *J. Exp. Bot.* **2016**, *67*, 2439–2451. [CrossRef]
18. Qiu, Z.; Yan, S.; Xia, B.; Jiang, J.; Yu, B.; Lei, J.; Chen, C.; Chen, L.; Yang, Y.; Wang, Y.; et al. The eggplant transcription factor MYB44 enhances resistance to bacterial wilt by activating the expression of *spermidine synthase*. *J. Exp. Bot.* **2019**, *70*, 5343–5354. [CrossRef]
19. Zhuo, T.; Wang, X.; Chen, Z.; Cui, H.; Zeng, Y.; Chen, Y.; Fan, X.; Hu, X.; Zou, H. The *Ralstonia solanacearum* effector RipI induces a defence reaction by interacting with the bHLH93 transcription factor in *Nicotiana benthamiana*. *Mol. Plant Pathol.* **2020**, *21*, 999–1004. [CrossRef]
20. Ashraf, M.F.; Yang, S.; Wu, R.; Wang, Y.; Hussain, A.; Noman, A.; Khan, M.I.; Liu, Z.; Qiu, A.; Guan, D.; et al. *Capsicum annuum HsfB2a* positively regulates the response to *Ralstonia solanacearum* infection or high temperature and high humidity forming transcriptional cascade with *CaWRKY6* and *CaWRKY40*. *Plant Cell Physiol.* **2018**, *59*, 2608–2623. [CrossRef]
21. Huang, J.; Shen, L.; Yang, S.; Guan, D.; He, S. CaASR1 promotes salicylic acid- but represses jasmonic acid-dependent signaling to enhance the resistance of *Capsicum annuum* to bacterial wilt by modulating CabZIP63. *J. Exp. Bot.* **2020**, *71*, 6538–6554. [CrossRef] [PubMed]
22. Chen, X.; Wang, W.; Cai, P.; Wang, Z.; Li, T.; Du, Y. The role of the MAP kinase-kinase protein StMKK1 in potato immunity to different pathogens. *Hortic. Res.* **2021**, *8*, 117. [CrossRef] [PubMed]
23. Wang, Y.; Zhao, A.; Morcillo, R.J.L.; Yu, G.; Xue, H.; Rufian, J.S.; Sang, Y.; Macho, A.P. A bacterial effector protein uncovers a plant metabolic pathway involved in tolerance to bacterial wilt disease. *Mol. Plant* **2021**, *14*, 1281–1296. [CrossRef] [PubMed]
24. Liu, Q.; Liu, Y.; Tang, Y.; Chen, J.; Ding, W. Overexpression of *NtWRKY50* increases resistance to *Ralstonia solanacearum* and alters salicylic acid and jasmonic acid production in tobacco. *Front. Plant Sci.* **2017**, *8*, 1710. [CrossRef]
25. Tang, Y.; Liu, Q.; Liu, Y.; Zhang, L.; Ding, W. Overexpression of *NtPR-Q* up-regulates multiple defense-related genes in *Nicotiana tabacum* and enhances plant resistance to *Ralstonia solanacearum*. *Front. Plant Sci.* **2017**, *8*, 1963. [CrossRef] [PubMed]
26. Liu, Y.; Liu, Q.; Tang, Y.; Ding, W. *NtPR1a* regulates resistance to *Ralstonia solanacearum* in *Nicotiana tabacum* via activating the defense-related genes. *Biochem. Biophys. Res. Commun.* **2019**, *508*, 940–945. [CrossRef] [PubMed]
27. Liu, Y.; Tang, Y.; Tan, X.; Ding, W. *NtRNF217*, encoding a putative RBR E3 ligase protein of *Nicotiana tabacum*, plays an important role in the regulation of resistance to *Ralstonia solanacearum* infection. *Int. J. Mol. Sci.* **2021**, *22*, 5507. [CrossRef] [PubMed]
28. Gao, W.; Chen, R.; Pan, M.; Tang, W.; Lan, T.; Huang, L.; Chi, W.; Wu, W. Early transcriptional response of seedling roots to *Ralstonia solanacearum* in tobacco (*Nicotiana tabacum* L.). *Eur. J. Plant Pathol.* **2019**, *155*, 527–536. [CrossRef]
29. Li, Y.; Wang, L.; Sun, G.; Li, X.; Chen, Z.; Feng, J.; Yang, Y. Digital gene expression analysis of the response to *Ralstonia solanacearum* between resistant and susceptible tobacco varieties. *Sci. Rep.* **2021**, *11*, 3887. [CrossRef]
30. Pan, X.; Chen, J.; Yang, A.; Yuan, Q.; Zhao, W.; Xu, T.; Chen, B.; Ren, M.; Geng, R.; Zong, Z.; et al. Comparative transcriptome profiling reveals defense-related genes against *Ralstonia solanacearum* infection in tobacco. *Front. Plant Sci.* **2021**, *12*, 767882. [CrossRef]
31. Alariqi, M.; Wei, H.; Cheng, J.; Sun, Y.; Zhu, H.; Wen, T.; Li, Y.; Wu, C.; Jin, S.; Cao, J. Large-scale comparative transcriptome analysis of *Nicotiana tabacum* response to *Ralstonia solanacearum* infection. *Plant Biotechnol. Rep.* **2022**, *16*, 757–775. [CrossRef]
32. Balakrishnan, D.; Surapaneni, M.; Mesapogu, S.; Neelamraju, S. Development and use of chromosome segment substitution lines as a genetic resource for crop improvement. *Theor. Appl. Genet.* **2019**, *132*, 1–25. [CrossRef] [PubMed]
33. Digonnet, C.; Martinez, Y.; Denance, N.; Chasseray, M.; Dabos, P.; Ranocha, P.; Marco, Y.; Jauneau, A.; Goffner, D. Deciphering the route of *Ralstonia solanacearum* colonization in *Arabidopsis thaliana* roots during a compatible interaction: Focus at the plant cell wall. *Planta* **2012**, *236*, 1419–1431. [CrossRef] [PubMed]
34. Bittner, R.J.; Arellano, C.; Mila, A.L. Effect of temperature and resistance of tobacco cultivars to the progression of bacterial wilt, caused by *Ralstonia solanacearum*. *Plant Soil* **2016**, *408*, 299–310. [CrossRef]
35. Caldwell, D.; Kim, B.S.; Iyer-Pascuzzi, A.S. *Ralstonia solanacearum* differentially colonizes roots of resistant and susceptible tomato plants. *Phytopathology* **2017**, *107*, 528–536. [CrossRef] [PubMed]
36. Li, Z.; Wu, S.; Bai, X.; Liu, Y.; Lu, J.; Liu, Y.; Xiao, B.; Lu, X.; Fan, L. Genome sequence of the tobacco bacterial wilt pathogen *Ralstonia solanacearum*. *J. Bacteriol.* **2011**, *193*, 6088–6089. [CrossRef] [PubMed]
37. Edwards, K.D.; Fernandez-Pozo, N.; Drake-Stowe, K.; Humphry, M.; Evans, A.D.; Bombarely, A.; Allen, F.; Hurst, R.; White, B.; Kernodle, S.P.; et al. A reference genome for *Nicotiana tabacum* enables map-based cloning of homeologous loci implicated in nitrogen utilization efficiency. *BMC Genom.* **2017**, *18*, 448. [CrossRef]
38. Kim, D.; Langmead, B.; Salzberg, S.L. HISAT: A fast spliced aligner with low memory requirements. *Nat. Methods* **2015**, *12*, 357–360. [CrossRef]

39. Pertea, M.; Pertea, G.M.; Antonescu, C.M.; Chang, T.C.; Mendell, J.T.; Salzberg, S.L. StringTie enables improved reconstruction of a transcriptome from RNA-seq reads. *Nat. Biotechnol.* **2015**, *33*, 290–295. [CrossRef]
40. Liao, Y.; Smyth, G.K.; Shi, W. featureCounts: An efficient general purpose program for assigning sequence reads to genomic features. *Bioinformatics* **2014**, *30*, 923–930. [CrossRef]
41. Love, M.I.; Huber, W.; Anders, S. Moderated estimation of fold change and dispersion for RNA-seq data with DESeq2. *Genome Biol.* **2014**, *15*, 550. [CrossRef] [PubMed]
42. Chen, C.; Chen, H.; Zhang, Y.; Thomas, H.R.; Frank, M.H.; He, Y.; Xia, R. TBtools: An integrative toolkit developed for interactive analyses of big biological data. *Mol. Plant* **2020**, *13*, 1194–1202. [CrossRef] [PubMed]
43. Finn, R.D.; Bateman, A.; Clements, J.; Coggill, P.; Eberhardt, R.Y.; Eddy, S.R.; Heger, A.; Hetherington, K.; Holm, L.; Mistry, J.; et al. Pfam: The protein families database. *Nucleic Acids Res.* **2014**, *42*, D222–D230. [CrossRef] [PubMed]
44. Paysan-Lafosse, T.; Blum, M.; Chuguransky, S.; Grego, T.; Pinto, B.L.; Salazar, G.A.; Bileschi, M.L.; Bork, P.; Bridge, A.; Colwell, L.; et al. InterPro in 2022. *Nucleic Acids Res.* **2023**, *51*, D418–D427. [CrossRef]
45. Finn, R.D.; Clements, J.; Eddy, S.R. HMMER web server: Interactive sequence similarity searching. *Nucleic Acids Res.* **2011**, *39*, W29–W37. [CrossRef] [PubMed]
46. Pfaffl, M.W. A new mathematical model for relative quantification in real-time RT-PCR. *Nucleic Acids Res.* **2001**, *29*, e45. [CrossRef] [PubMed]
47. Senthil-Kumar, M.; Mysore, K.S. Tobacco rattle virus-based virus-induced gene silencing in *Nicotiana benthamiana*. *Nat. Protoc.* **2014**, *9*, 1549–1562. [CrossRef] [PubMed]
48. Kang, Y.; Lee, K.; Hoshikawa, K.; Kang, M.; Jang, S. Molecular bases of heat stress responses in vegetable crops with focusing on heat shock factors and heat shock proteins. *Front. Plant Sci.* **2022**, *13*, 837152. [CrossRef]
49. Neves, C.; Ribeiro, B.; Amaro, R.; Exposito, J.; Grimplet, J.; Fortes, A.M. Network of GRAS transcription factors in plant development, fruit ripening and stress responses. *Hortic. Res.* **2023**, *10*, uhad220. [CrossRef]
50. Aldon, D.; Mbengue, M.; Mazars, C.; Galaud, J.P. Calcium signalling in plant biotic interactions. *Int. J. Mol. Sci.* **2018**, *19*, 665. [CrossRef]
51. Suleman, M.; Ma, M.; Ge, G.; Hua, D.; Li, H. The role of alternative oxidase in plant hypersensitive response. *Plant Biol.* **2021**, *23*, 415–419. [CrossRef] [PubMed]
52. Yu, T.Y.; Sun, M.K.; Liang, L.K. Receptors in the induction of the plant innate immunity. *Mol. Plant. Microbe Interact.* **2021**, *34*, 587–601. [CrossRef] [PubMed]
53. Luo, D.; Wu, Z.; Bai, Q.; Zhang, Y.; Huang, M.; Huang, Y.; Li, X. Universal stress proteins: From gene to function. *Int. J. Mol. Sci.* **2023**, *24*, 4725. [CrossRef] [PubMed]
54. Li, W.; Zheng, X.; Cheng, R.; Zhong, C.; Zhao, J.; Liu, T.H.; Yi, T.; Zhu, Z.; Xu, J.; Meksem, K.; et al. Soybean ZINC FINGER PROTEIN03 targets two *SUPEROXIDE DISMUTASE1s* and confers resistance to *Phytophthora sojae*. *Plant Physiol.* **2023**, *192*, 633–647. [CrossRef] [PubMed]
55. Kunkel, B.N.; Harper, C.P. The roles of auxin during interactions between bacterial plant pathogens and their hosts. *J. Exp. Bot.* **2018**, *69*, 245–254. [CrossRef] [PubMed]
56. Kunkel, B.N.; Johnson, J.M.B. Auxin plays multiple roles during plant–pathogen interactions. *Cold Spring Harb. Perspect. Biol.* **2021**, *13*, a040022. [CrossRef] [PubMed]
57. Wan, J.; He, M.; Hou, Q.; Zou, L.; Yang, Y.; Wei, Y.; Chen, X. Cell wall associated immunity in plants. *Stress Biol.* **2021**, *1*, 3. [CrossRef]
58. Bacete, L.; Melida, H.; Miedes, E.; Molina, A. Plant cell wall-mediated immunity: Cell wall changes trigger disease resistance responses. *Plant J.* **2018**, *93*, 614–636. [CrossRef]
59. Bacete, L.; Hamann, T. The role of mechanoperception in plant cell wall integrity maintenance. *Plants* **2020**, *9*, 574. [CrossRef]
60. Barnes, W.J.; Anderson, C.T. Release, recycle, rebuild: Cell-wall remodeling, autodegradation, and sugar salvage for new wall biosynthesis during plant development. *Mol. Plant* **2018**, *11*, 31–46. [CrossRef]
61. Tucker, M.R.; Lou, H.; Aubert, M.K.; Wilkinson, L.G.; Little, A.; Houston, K.; Pinto, S.C.; Shirley, N.J. Exploring the role of cell wall-related genes and polysaccharides during plant development. *Plants* **2018**, *7*, 42. [CrossRef] [PubMed]
62. Shi, H.; Liu, Y.; Ding, A.; Wang, W.; Sun, Y. Induced defense strategies of plants against *Ralstonia solanacearum*. *Front. Microbiol.* **2023**, *14*, 1059799. [CrossRef] [PubMed]
63. Ul Haq, S.; Khan, A.; Ali, M.; Khattak, A.M.; Gai, W.X.; Zhang, H.X.; Wei, A.M.; Gong, Z.H. Heat shock proteins: Dynamic biomolecules to counter plant biotic and abiotic stresses. *Int. J. Mol. Sci.* **2019**, *20*, 5321. [CrossRef] [PubMed]
64. Saibil, H. Chaperone machines for protein folding, unfolding and disaggregation. *Nat. Rev. Mol. Cell Biol.* **2013**, *14*, 630–642. [CrossRef] [PubMed]
65. Kim, T.; Samraj, S.; Jimenez, J.; Gomez, C.; Liu, T.; Begcy, K. Genome-wide identification of heat shock factors and heat shock proteins in response to UV and high intensity light stress in lettuce. *BMC Plant Biol.* **2021**, *21*, 185. [CrossRef]
66. Nagaraju, M.; Kumar, A.; Jalaja, N.; Rao, D.M.; Kishor, P.B.K. Functional exploration of chaperonin (HSP60/10) family genes and their abiotic stress-induced expression patterns in *Sorghum bicolor*. *Curr. Genom.* **2021**, *22*, 137–152. [CrossRef]
67. Wu, J.; Gao, T.; Hu, J.; Zhao, L.; Yu, C.; Ma, F. Research advances in function and regulation mechanisms of plant small heat shock proteins (sHSPs) under environmental stresses. *Sci. Total Environ.* **2022**, *825*, 154054. [CrossRef]

68. Berka, M.; Kopecka, R.; Berkova, V.; Brzobohaty, B.; Cerny, M. Regulation of heat shock proteins 70 and their role in plant immunity. *J. Exp. Bot.* **2022**, *73*, 1894–1909. [CrossRef]
69. Han, Z.; Xiong, D.; Schneiter, R.; Tian, C. The function of plant PR1 and other members of the CAP protein superfamily in plant–pathogen interactions. *Mol. Plant Pathol.* **2023**, *24*, 651–668. [CrossRef]